ELSEVIER

Ceramics International 28 (2002) 627–636

CERAMICS INTERNATIONAL

www.elsevier.com/locate/ceramint

Structural characterization and mixed conductivity of TiO_2-doped ceria stabilized tetragonal zirconia☆

F. Capel, C. Moure, P. Durán*

Instituto de Cerámica y Vidrio (CSIC), Departamento de Electrocerámica, 28500-Arganda del Rey, Madrid, Spain

Received 27 September 2001; received in revised form 10 October 2001; accepted 7 November 2001

Abstract

By using X-ray diffraction lattice parameter measurements and Raman spectroscopy studies, the solid solubility limits of titania in ceria tetragonal zirconia solid solutions (12 mol% CeO_2) have been established. Electrical properties of the mixed conductor TiO_2–Ce–TZP containing 5 and 10 mol% TiO_2 were measured at the 300 °C–900 °C temperature range. The total electrical conductivity in air of the TiO_2–Ce–TZP ceramics decreases with titania content due to Ti-Vö associations, which depresses the mobility of the oxygen vacancies during the conduction process. The electrical behaviour of undoped-Ce–TZP solid solutions as a function of the pO_2 and temperature showed that in oxidising conditions and up to an oxygen partial pressure of 10^{-9} Pa the materials were nearly pO_2 independent. Under lower oxygen partial pressure the total electrical conductivity increases according to $pO_2^{-1/6}$ indicating that the *n*-type conduction in Ce–TZP is due to the electron hopping between Ce^{4+} and Ce^{3+} cations. In Ce–TZP containing 5 and 10 mol% titania the electrical behaviour was very different mainly under the most reducing conditions. Above 800 °C and with decreasing oxygen partial pressure below 10^{-9} Pa, the theoretical correlation for electronic conduction was near to $n \propto pO_2^{-1/4}$, which indicates that the conduction process is controlled by the Ce'_{Zr} and Ti'_{Zr} defect concentrations, by hopping of the electrons between Ce^{4+} and Ce^{3+} and Ti^{4+} and Ti^{3+} via a small polaron hopping mechanism. © 2002 Published by Elsevier Science Ltd and Techna S.r.l.

Keywords: Lattice parameter; Raman spectroscopy; Mixed conductivity; Tetragonal zirconia; XPS

1. Introduction

It is well known that mixed (ionic and electronic) ceramic conductors offer potential applications as oxygen semipermeable membranes in those processes involving oxygen extraction at high temperature [1–3]. For example, in the particular case of production of H_2 or CO by thermal dissociation of H_2O or CO_2 [4], it has been previously established that at the required temperatures for the above reaction, and in an oxygen partial pressure range of 10^{-3}–10^{-7}, the material used as semipermeable membrane should have a mixed electrical conductivity with the same order of magnitude for both ionic and electronic conductivity. In those conditions the oxygen transfer is maximum between the electrolyte and the gaseous species [5].

In order to optimise the role of the electrodes, i.e. the catalytic activity, used in a SOFC system, many perovskite oxides as for example $Ln_{1-x}Sr_x$ MnO_3 and $Ln_{1-x}Sr_xCoO_3$ have been suggested. However their performances are strongly limited due to the high reactivity of both with the YSZ electrolyte, leading to the formation of secondary phases like $La_2Zr_2O_7$ which is a poorly conducting phase [6]. As an alternative, a monolithic structural has recently been proposed in which the single crystalline structure phase, $Gd_2(Ti_{1-x}Ru_x)_2O_7$ (Cathode)/$(Gd_{1-x}Ca_x)_2Ti_2O_7$ (electrolyte)/$Gd_2(Ti_{1-x}Mo_x)_2O_7$ (anode), serves as a template for the cell [7,8].

There is a general consensus that, from an electrical behaviour point of view, mixed ionic and electronic conductors could be the best kind of electrode materials for SOFC and electrolyser. Nevertheless other requirements such as thermal stability, good matching with the thermal expansion coefficient of the electrolyte, and

☆ Based on a part of the PhD thesis of F. Capel, Universidad Complutense of Madrid, 1998.

* Corresponding author. Tel.: +34-91-8711800; fax: +34-91-8700550.

E-mail address: pduran@icv.csic.es (P. Durán).

0272-8842/02/$22.00 © 2002 Published by Elsevier Science Ltd and Techna S.r.l.
PII: S0272-8842(02)00019-6

over all chemical compatibility with the electrolyte at the operation temperatures of the SOFC, have to be fulfilled. On that basis, other electrode materials such as ceramics based on CeO_2 have recently been proposed [9]. The main problem of such a ceramic electrode was its cracking and spalling from the electrolyte substrate when cycling between reducing and oxidising conditions. Therefore the search of new ceramic materials to be used as electrodes, mainly oxide anodes, in SOFCs systems is currently under investigation in many laboratories.

The aim of this work is to study the structure and the electrical behaviour of TiO_2 doped-ceria stabilised tetragonal zirconia in air and in reducing conditions in order to know the TiO_2 doping effects on ionic and electronic conductivity at the SOFC operating temperatures of 700–900 °C.

2. Experimental procedure

Ce–TZP powders (12 mol%) with TiO_2 content ranging 0–10 mol% were prepared by coprecipitation of the hydroxides, from an aqueous solution containing the appropriate amounts of $CeCl_3{\cdot}H_2O$, $ZrOCl{\cdot}H_2O$ and $Ti(C_5H_9O)_4$ C_5H_9OH, with ammonia. After drying at 120 °C in air overnight, the powders were ball-milled in methanol for 2 h, redried at 80 °C for 5 h, and calcined at 1300 °C for 2 h. After calcining the powders were ground, isopressed at 200 MPa, and sintered at 1400 °C for 5 h in air. The crystal structures of the sintered samples were studied using an X-ray diffractometer (Siemens D-5000), with CuK_α radiation measuring the variation of the lattice parameters, a and c, with increasing titania content.

Polarized Raman spectra were measured at 300 K in a backscattering geometry, in a Dilor XY spectrometer with diode array multichannel detector and a ×50 microscope objective lens. The light power at the sample was of the order of 150 mW and the spectral resolution better than 2 cm^{-1}. The samples were excited with the 496.5 nm Ar^+ laser.

X-ray photoelectron spectroscopy studies were performed in an ultrahigh vacuum system (base pressure of 4×10^{-9} mbar). Spectra were obtained using an electron spectrometer with a hemispherical analyzer and a Mg$K\alpha$ X-ray source (120 W). Details have been described elsewhere [10].

Platinum paste (Engelhard 6082) was painted on both sides of the sintered discs and dried in an oven at 120 °C to eliminate the solvent. After drying, the electrode samples were annealed at 800 °C for a short time, about 30 min, to avoid an excessive shrinkage of the platinum electrodes. To these electrodes samples were welded platinum lead wire and placed in the hot zone of a programmed furnace with a chromel–alumel thermocouple located on the mid-point of the electrode sample.

The temperature dependence of electrical conductivity was measured by using an impedance Analyzer (Hewlett-Packard model 4192A) in the frequency range of 5 Hz to 13 MHz. Measurements were made in air in the temperature range of 200–800 °C. For comparison, an undoped Ce–TZP sample sintered in the same conditions as for TiO_2-doped ones was used.

The dependence of electrical conductivity on the oxygen partial-pressure was also measured in the oxygen partial-pressure range 0.21–10^{-18} atm and in the temperature range of 700–900 °C. The experiments were performed in a controlled atmosphere furnace using a YSZ sensor and one YSZ electrochemical pump as detailed elsewhere [11].

3. Experimental results

3.1. Structural characterization

The lattice parameters a and c of tetragonal zirconia decreased and increased, respectively, with increasing TiO_2 concentration and appear to reach a constant value at about 10 mol% TiO_2 [10]. The variation of the tetragonality c_t/a_t as a function of the TiO_2 content can be seen in Fig. 1. As shown, the tetragonality remains constant beyond 10 mol% TiO_2, confirming the statement for the solubility limit for TiO_2 in tetragonal zirconia. These results are consistent with the scanning electron microscopy (SEM) observations, see Fig. 2a and b, in which a composition containing 15 mol% TiO_2 showed a considerable amount of a second phase, the zirconium titanate (ZT), which favored grain growth. The pyrochlore phase ($Zr_2Ce_2O_7$) was not detected. Therefore, the solubility limit of TiO_2 into tetragonal zirconia is well bellow 12 mol% TiO_2 up to

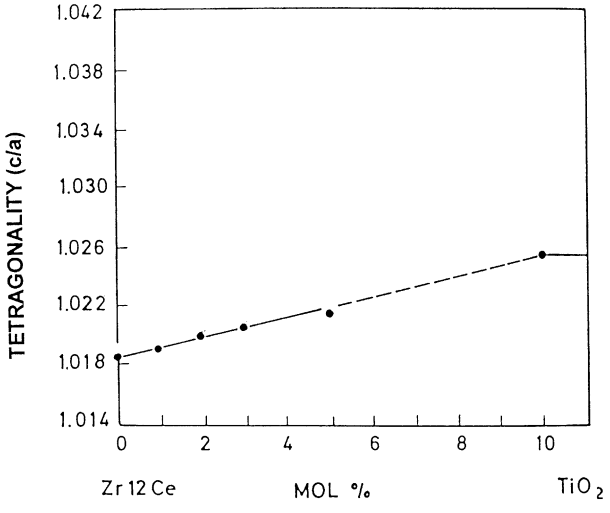

Fig. 1. Tetragonality (c/a) shift versus TiO_2 content of sintered samples.

1400 °C and confirm the data reported elsewhere for the ZrO_2–CeO_2–TiO_2 system [12].

Fig. 3 shows the Raman spectra obtained from samples as a function of the TiO_2 content. The Raman spectrum of tetragonal zirconia exhibits six active modes which can be attributed to the Zr–O_I stretching lines at 634 and 600 cm^{-1}, to the coupling of O_I (or O_{II})–Zr–O_I (or O_{II}) bending and of Zr–O_I and Zr-O_{II} stretching, the 459 and 318 cm^{-1} lines. The line at 257 cm^{-1} is mainly attributed to Zr–O_{II} stretching and the band at 143 cm^{-1} to O_I–Zr–O_I and Zr–O_I–Zr bending. As it can be seen from the Fig. 3, among the six Raman modes only those near 257 and 634 cm^{-1} continuously move to higher frequencies as the TiO_2 content increases. The shifts of the 257 cm^{-1} mode of were much greater than that of the 634 cm^{-1} one. Given that these bands correspond to the Zr-O_{II} and Zr-O_I stretching modes; then, both the cation-O_{II} and the cation-O_I bond lengths in are modified with increasing TiO_2 content.

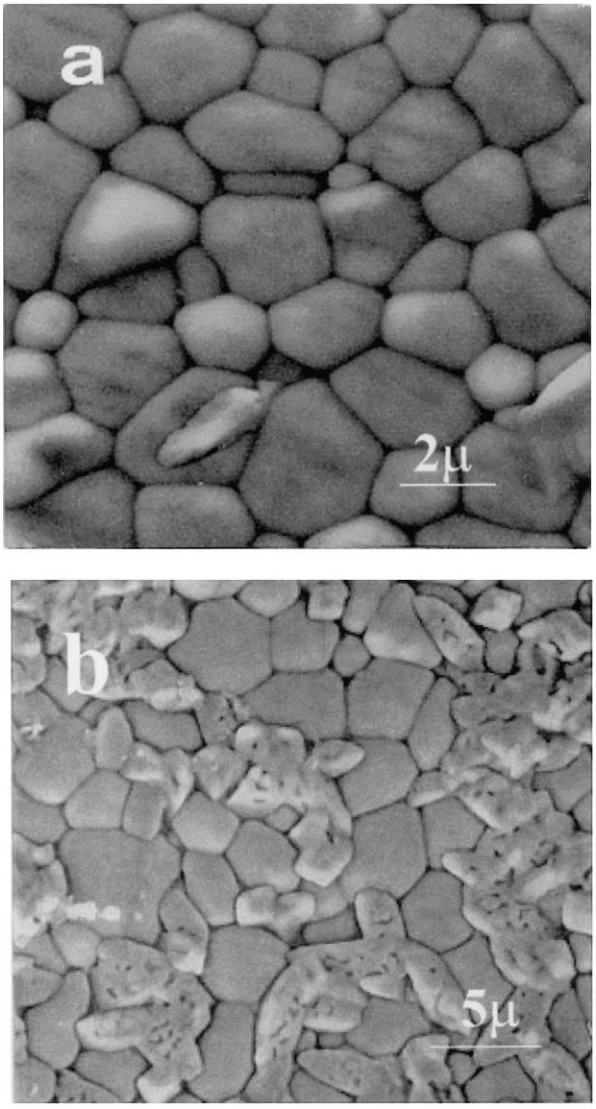

Fig. 2. SEM microstructure of (a) 10TiO_2- and (b) 15TiO_2-sintered samples showing a zirconium titanate second phase.

The zirconia–oxygen bond lengths in Ce–TZP can be easily estimated from the precision lattice parameter measurements [13]. The calculated values for Ce–TZP and TiO_2-doped solid solutions are listed in Table 1. A slight decrease or increase for Zr–O_I and Zr–O_{II} bond lengths, respectively, occurs in Ce–TZP as a result of the increased TiO_2 content introduced in the tetragonal matrix. These results confirm the statement that the Raman shift toward greater frequencies of only the 634 and 257 cm^{-1} modes are closely related to a modification of the Zr–O_I and Zr–O_{II} bond lengths. Such a selective shift in the Raman modes in Fig. 3 indicates that the local environment of the tetravalent cations Ti^{4+} to O^{2-} in the ZrO_2–CeO_2–TiO_2 system can be different from that of cations in the binary ZrO_2–CeO_2 one, where cations are eightfold co-ordinated. Given that the ionic radius of Ti^{4+} for sixfold co-ordination is 0.074 nm, it is most likely that the selective Raman shifts arise from the occupation of the tetravalent ions Ti^{4+} in distorted sites in the tetragonal zirconia crystal lattice [10].

The MgK_α XPS spectra for the Ce3d core level showed three clear peaks at about 882.8, 900 and 916.7 eV which can be attributed to the binding energies of Ce^{4+} $3d_{5/2}$ and Ce^{4+} $3d_{3/2}$, respectively. The peak which appear at about 884.3 eV can be attributed to the binding energy of the Ce^{3+} $3d_{5/2}$, see Fig. 4. The binding energy of these peaks are in good agreement with the binding energy given by other authors [14], and it allows one to suggest the presence of Ce^{4+} and Ce^{3+} in the Ce–TZP and TiO2-doped Ce–TZP sintered samples.

The MgK_α XP spectrum for the Ti 2p core level, not shown here, showed two peaks at binding energies of 458.5 and 464.2 eV which correspond to Ti $2p_{3/2}$ and Ti $2p_{1/2}$, respectively, for Ti^{4+}. Peaks for Ti^{3+}, if any, should appear at energies of 457.2 and 463.0 eV. Therefore, no evidence for the presence of reduced Ti^{3+} was found from XPS results on the TiO_2-doped samples sintered at 1400 °C in air. Table 2 summarises the binding energy values for O1s, $Zr3d_{5/2}$, $Ce3d_{5/2}$ and $Ti2p_{3/2}$.

Table 1
Calculated Zr-O bond lengths as a function of TiO_2 content

Composition (mol%)			Length (nm)	
ZrO_2	CeO_2	TiO_2	Zr–O_I	Zr–O_{II}
88	12		0.2098	0.2380
87	12	1	0.2096	0.2390
86	12	2	0.2094	0.2393
85	12	3	0.2093	0.2396
83	12	5	0.2087	0.2399
78	12	10	0.2074	0.2411

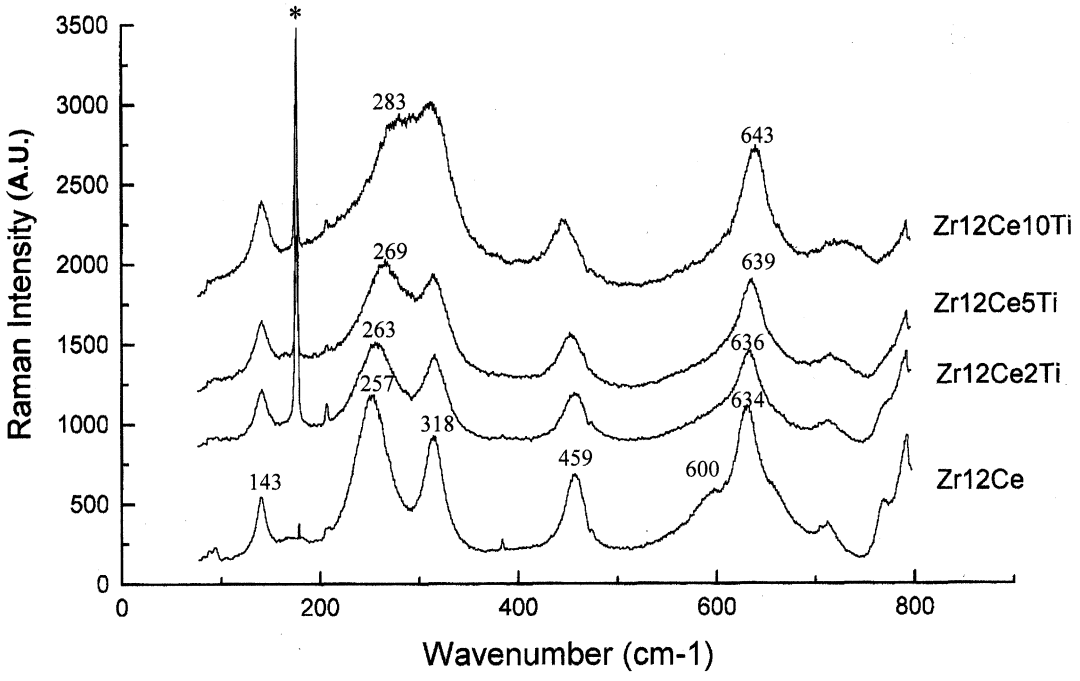

Fig. 3. Raman spectra of sintered samples with different TiO_2 contents at room temperature.

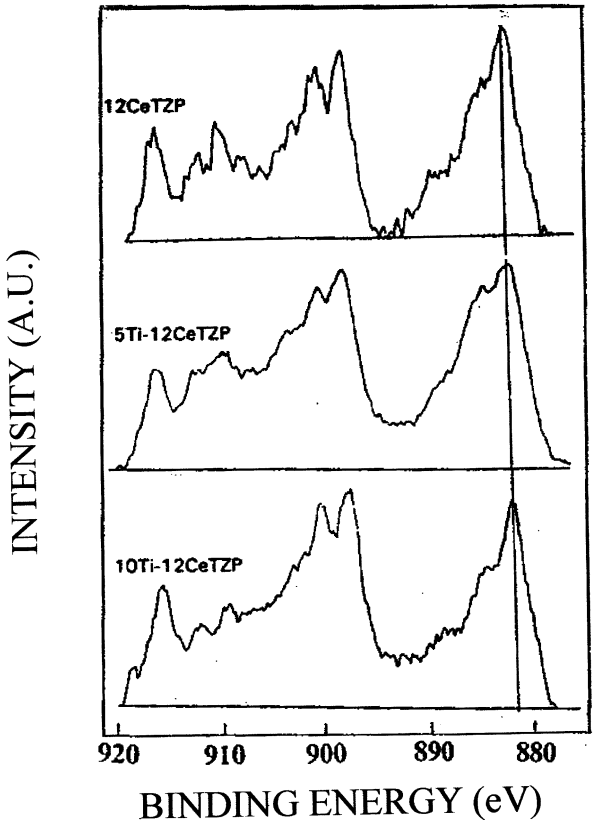

Fig. 4. Ce 3d electron spectra of TiO_2- solid solutions sintered in air.

3.2. Total electrical conductivity in air

The ac conductivity results were plotted in the complex impedance plane, and the typical ac impedance spectra obtained as a function of the temperature for titania-doped tetragonal zirconia (5Ti–Ce–TZP) are shown in Fig. 5. It appears that the grain boundary contribution to the total conductivity is much lower than that of the lattice conductivity one, which indicates that grain size increase with TiO_2 content [10]. In order to elucidate the mechanism for conduction the Fig. 6 shows the conductivity as a function of temperature. From the slope of these curves the conduction activation energies were calculated which are summarised in Table 3. In all the cases single activation energy was found for the temperature range studied. The calculated

Table 2
Binding energies (eV) of photoelectrons O1s, Zr3d, Ce3d and Ti2p of ZrO_2–CeO_2–TiO_2 system

MUESTRA	O1s	$Zr3d_{5/2}$	$Ce3d_{5/2}$	$Ti2p_{3/2}$
12Ce–TZP	530.2 (50) 532.2 (50)	182.3	882.3	–
5Ti-12Ce–TZP	530.2 (56) 532.2 (44)	182.3	882.4	458.6
10Ti–12Ce–TZP	530.1 (44) 532.0 (56)	182.3	882.4	458.7

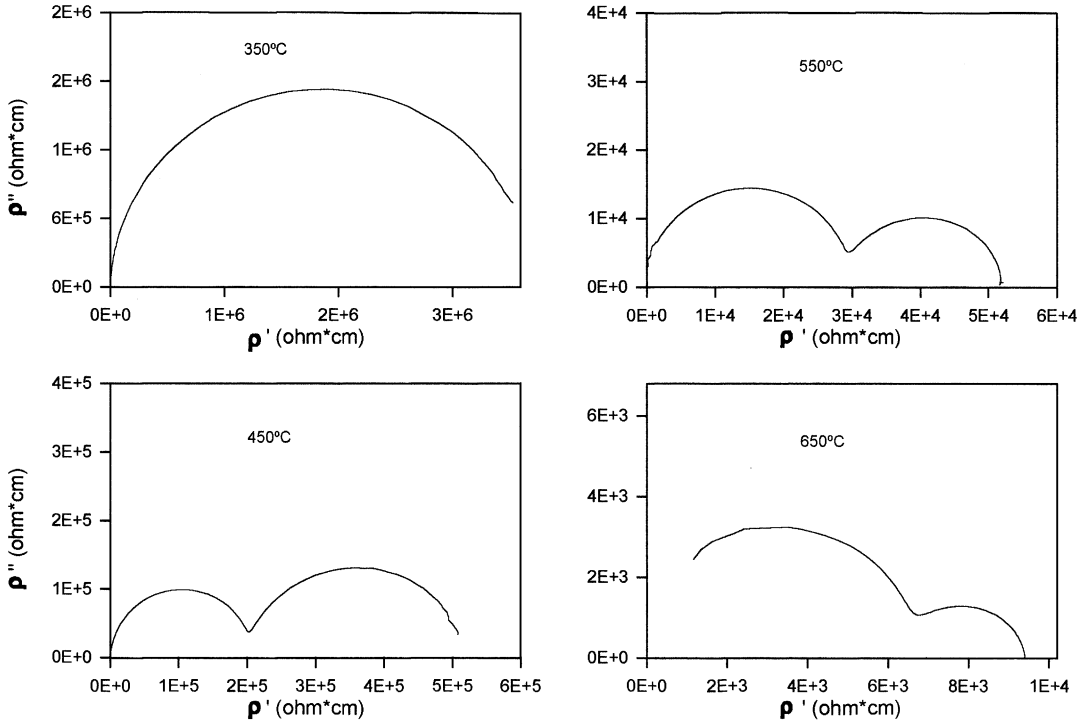

Fig. 5. Typical complex impedance plot for the sample $5TiO_2$ at the indicated temperatures.

activation energies were in the order of 1.0 ± 0.1 eV which coincides well with that corresponding to the activation energy for oxygen vacancy conduction [15]. However, in order to know what is the predominant conduction mechanism, an attempt to calculate the bulk and grain boundary conductivity at that temperature range above 400 °C, in which both the bulk and grain boundary semicircles were well developed was made. With these conductivity data and assuming that the electrical conductivity follows an Arrhenius equation of the type:

$$\sigma = \sigma_o exp(-Ea/RT) \quad (1)$$

where T is the absolute temperature, σ_o is a constant, E_a is the activation energy for the motion of charges, and R is the gas constant, the temperature dependence of the bulk, grain boundary, and total conductivity for 5Ti-Ce–TZP, 10Ti-Ce–TZP, and undoped samples was studied. In Table 3 the activation energy values for the three samples in the temperature range of 400–900 °C are shown.

From the Arrhenius plot a general trend to decrease the electrical conductivity with increasing titania content up to 10 mol%, as shown in Fig. 6, can be observed. Titania concentration higher than 10 mol% decreased the electrical conductivity as consequence of the appearance of a second phase (ZT). From these data and the similar activation energy value for the bulk and total conductivity processes allows one to assume that a

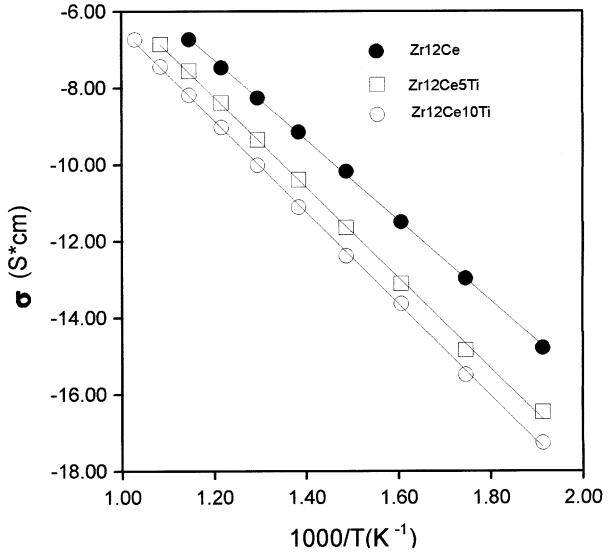

Fig. 6. Arrhenius plot of total conductivity of TiO_2–solid solutions in air.

Table 3
Activation energy values (eV) for the conductivity of tetragonal zirconia samples

Sample	E_B	E_{GB}	E_T
Ce–TZP	0.86	1.02	0.90
5Ti–Ce–TZP	0.98	1.13	1.02
10Ti–Ce–TZP	1.03	1.16	1.04

bulk oxygen ion transport seems to be predominant in the air sintered samples studied.

3.3. Total electrical conductivity under reducing atmospheres

The oxygen partial-pressure dependence of total electrical conductivity in Ce–TZP and Ce–TZP containing 5 and 10 mol% TiO_2 are shown in Fig. 7a–c, respectively. From the Fig. 7a, it seems clear that sample displayed a behaviour with two well-established zones within the experimental temperature range. The first one in which the total conductivity is independent of the oxygen activity and is given by the concentration of oxygen vacancies [Vö] provided by the amount of CeO_2 reduced to Ce_2O_3, and introduced into the zirconia according to the following hypothetical reaction:

$$Ce_2O_3 \rightleftharpoons 2Ce'_{Zr} + V\ddot{o} + 3O_o^x \quad (2)$$

where Kroger's notations have been used [16]. The total electrical conductivity at this zone is mainly ionic conductivity and is currently named as ionic domain. As it can be observed, the domain range decreases with increasing temperature and titania content.

Beyond the limits of the ionic domain, a second zone is observed in which a rapid increase of the total electrical conductivity takes place. The slopes of the log σ vs. log pO_2 curves within the experimental temperature range were near to –1/6. Such an increasing is due to the contribution of the electronic conductivity as consequence of the reduction of a higher amount of CeO_2. Then the following reaction must be taken into account [17]:

$$2Ce_{Zr}^x + O_o^x \rightleftharpoons 2Ce'_{Zr} + V\ddot{o} + 1/2O_2(g) \quad (3)$$

where $Ce^x{}_{Zr}$ is a Ce^{4+} cation and Ce'_{Zr} is a reduced Ce^{3+} cation. According to Eq. (3), the reduction of Ce^{4+} is accompanied by the formation of oxygen vacancies and is the responsible of the ionic domain, in which the oxygen vacancies concentration can be considered as constant for each temperature, and whose extension depends, therefore, on the redox equilibrium between tetravalent Ce^{4+} and trivalent Ce^{3+} cations. In the measure to which the electronic contribution becomes more noticeable the total electrical conductivity should increase.

In the case of the 5Ti–Ce–TZP and 10Ti–TZP samples, a third zone in which the electronic contribution is dominant appeared for the lower oxygen partial pressure. Such a zone is characterised by a slight decrease of the total electrical conductivity, which is proportional, as in the second zone, to $pO_2^{-1/n}$. The negative slope of the oxygen dependent regions suggested *n*-type semiconduction.

Although the same two different zones appeared in Fig. 7b and c, the TiO_2-doped samples displayed distinct slopes in the *n*-type zone with increasing temperature and lower oxygen partial pressure. As it can be observed, the slope was not close to –1/6 but it deviated towards higher values. An explanation can be attained as follows; if the law of mass action is applied to Eq. (3), the following relation is obtained:

$$K = [\ Ce'_{Zr}\ ]^2[\ V\ddot{o}\ ]pO_2 \quad (4)$$

or

$$K = n^2[\ V\ddot{o}\ ]pO_2 \quad (5)$$

if, in first-order approximations, the activity and the concentration of a given species are considered to be equal. In that equation n is the electron concentration and pO_2 the equilibrium oxygen partial pressure.

To satisfy the electrical neutrality for the tetragonal zirconia solid solutions, the following condition has to be considered

$$2[V\ddot{o}\ ] = [\ Ce'_{Zr}\ ] + n \quad (6)$$

Since the total conductivity σ is given by

$$\sigma = [\ V\ddot{o}\ ]2q\mu_{V\ddot{o}} + [\ Ce'_{Zr}\ ]nq\mu_{e'} \quad (7)$$

where $\mu_{V\ddot{o}}$, and $\mu_{e'}$ are the oxygen vacancy, and electron mobility, respectively, and q is the electronic charge. The total conductivity will be determined by the relative ionic and electronic contributions, and hence by the concentrations of charge carriers and their corresponding mobilities. Combining Eqs. (5)–(7) and at low enough oxygen partial pressures, we obtain the following relations for the total electrical conductivity:

$$\sigma \propto pO_2{}^{-1/4} \quad (8)$$

and

$$\sigma \propto pO_2{}^{-1/6} \quad (9)$$

for $n << [Ce'_{Zr}]$ or $n >> [Ce'_{Zr}]$, respectively.

It must be noted that while in the undoped-tetragonal zirconia the concentration of electronic charge carriers, *n*, correlated well to $pO_2^{-1/6}$ in the case of the TiO_2-doped tetragonal zirconia samples the theoretical correlation of n is nearly to $pO_2^{1/4}$. These results indicated that the created electrons induce the electronic conduction (*n*-type) not only as consequence of the reduction of the $Ce^{4+} \rightarrow Ce^{3+}$ but also of $Ti^{4+} \rightarrow Ti^{3+}$. These electrons, being located on cerium and titanium sites move in the lattice by jump between Ce^{4+} and Ce^{3+} and between Ti^{4+} and Ti^{3+} cations. Such an *n*-type

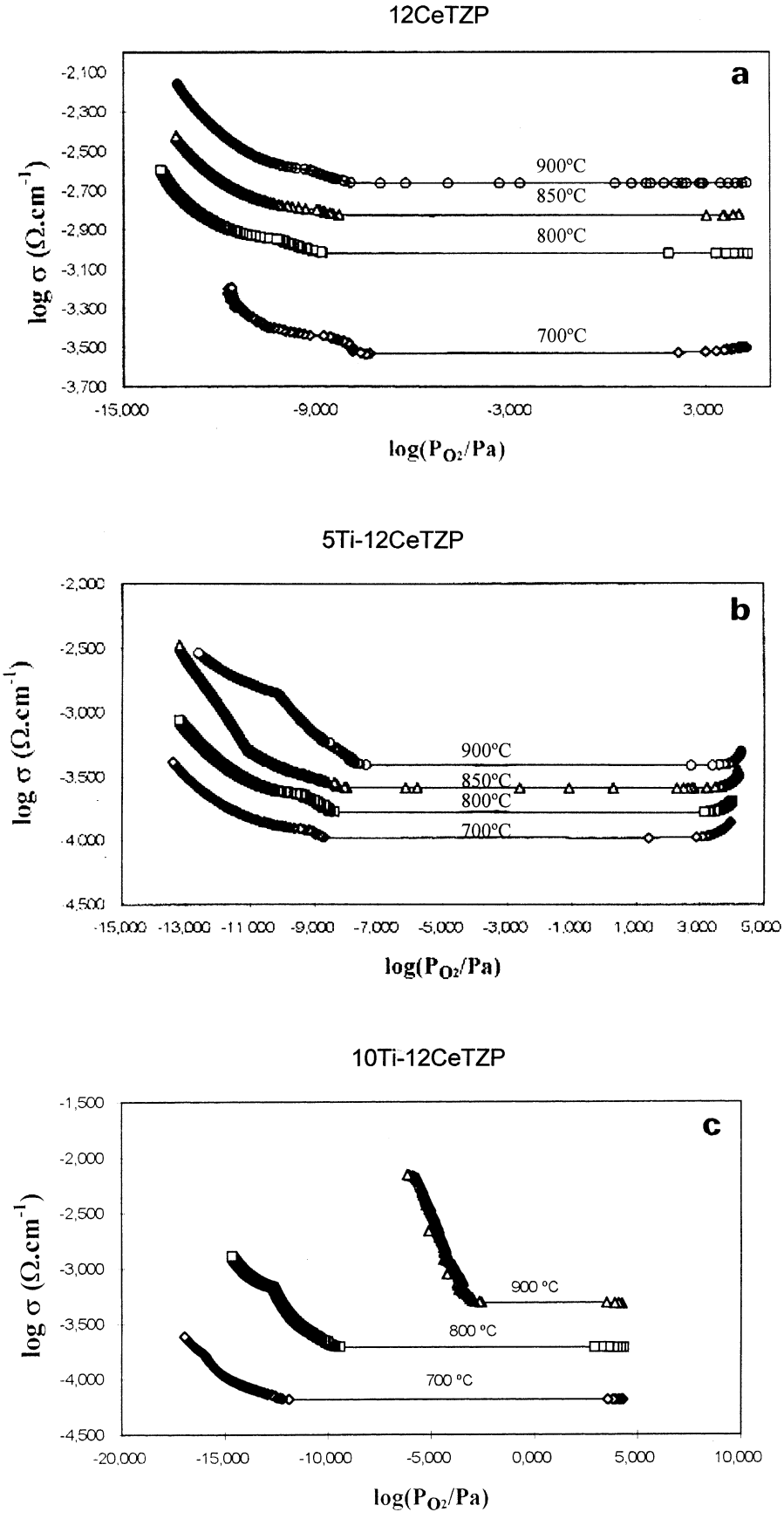

Fig. 7. Oxygen partial pressure dependence of electrical conductivity of TiO_2-solid solutions at different temperatures.

conduction observed in TiO_2–Ce–TZP was also found in Me-doped YSZ (Me = Ti, Ce, Tb) [2,18,19], and in CeO_2-based ceramics [20] and was attributed to a small polaron-hopping mechanism.

4. Discussion

From the X-ray diffraction lattice parameter measurements and Raman spectroscopy results (see Figs. 1 and 3), it can be stated that the solubility limit for titania in tetragonal zirconia (12 mol% CeO_2) up to 1400 °C is close to ~10 mol%. Compositions containing higher titania content showed the incipient presence of a second phase, the zirconium titanate (ZT), in agreement with that established for ZrO_2–CeO_2–TiO_2 binary system [12].

It was also noticed that the tetragonality, c/a, of the zirconia solid solutions increases with increasing TiO_2 content, see Fig. 1, and this became constant for a TiO_2 content about 10 mol%, confirming the statement for the solubility limit of TiO_2 in tetragonal zirconia. This solid solution with a tetragonality of about 1.0252, much higher than that of the binary tetragonal zirconia-ceria solid solution [21], 1.0178, was also stable at room temperature. Such an enhanced stability can be attributed to the high bonding anisotropy produced as consequence of the introduction of Ti^{4+} into the layer-like zirconia structure. Given that the size of the Ti^{4+} cation ($R_{Ti4+} = 0.745$ Å) is much smaller than Zr^{4+} ($R_{Zr4+} = 0.86$ Å) it could adopt a lower co-ordination which would favour a packing in the form of a relatively ordered layer-like structure. This could alleviate the oxygen overcrowding around Zr cations, similarly to that occurring in GeO_2-doped tetragonal zirconia [22]. A Ti cationic short-range ordering was also detected by TEM in the ZrO_2–CeO_2–TiO_2 system for a stable composition having tetragonality as high as 1.032 [23]. If this is so then such a Ti cationic ordering could reduce the strain energy of the tetragonal lattice, leading to a higher stability of the titania-doped tetragonal zirconia solid solutions. It seems clear from the calculated zirconium-oxygen bond lengths in TiO_2-doped solid solutions, see Table 1, that the local bonding environment of the tetravalent cations Ti^{4+} to O^{2-} in the ZrO_2–CeO_2–TiO_2 system is different from that of cations in the binary ZrO_2–CeO_2 one, where cations are eight-fold co-ordinated, leading to assume a co-ordination for Ti^{4+} cations lower than eight-fold [24].

The electrical behaviour of TiO_2-doped tetragonal zirconia solid solutions shows the same dependence, as reported by Arashi and Naito [25] and Duran et al. [24] for the case of TiO_2-YTZP solid solutions, i.e. the electrical conductivity in air decreases with titania content. Such an electrical conductivity takes place, according to the activation energy values reported for the total conductivity process, by a bulk oxygen transport as the predominant mechanism. Given that the ionic radius of Ce^{3+} ion compares well with that of yttrium as dopant, a similar explanation can be made for such an electrical behaviour taking into account the Li et al. [22] model, and assuming that the oversized Ce^{3+} cations substitute for Zr^{4+} in the cation network, adopting a CeO_8 structure. If this would be so, then the Ce^{3+} cations will not be associated with oxygen vacancies, given that those eightfold doping co-ordination leaves oxygen vacancies near to the both Zr and Ti cations. Therefore, the Zr (Ti)-vacancy pairing would be energetically more favourable than Ce-vacancy pairing in Ce-doped zirconia as previously suggested [22]. In that situation, an undersized tetravalent doping as the Ti^{4+} cations, which do not substitute random by for Zr cations in tetragonal zirconia solid solutions [24] and, probably, adopting a co-ordination number smaller than eight-fold, will be in competition with Zr cations for the oxygen vacancies. On that basis, two kind of vacancy (Vö)-cation associations have to be formed, one of them Zr–Vö in which the oxygen vacancy is associated to a cation octahedrally co-ordinated. The other one would be Ti–Vö with oxygen vacancy associated to a cation with a smaller co-ordination number according to the following reactions:

$$Ce_2O_3(TiO_2) \xrightarrow{ZrO_2} Ce'_{Zr} + Ti_{Zr} + V\ddot{o} + 5O_o$$

$$Ti'_{Zr} + V\ddot{o} \rightleftharpoons Ti'_{Zr}\ V\ddot{o}$$

$$Zr_{Zr} + V\ddot{o} \rightleftharpoons Zr_{Zr}\ V\ddot{o}$$

This being so, then it must be also assumed two oxygen sublattices with different vacancy diffusion dynamics. Since the Ti-O distances are shorter than the Zr-O ones, we can state a more rapid oxygen vacancy diffusion on the octahedrally co-ordinated sublattice leading, thus, to a hindering (trapping) for the global mobility of the oxygen vacancies by the presence of the Ti ions in the TiO_2-doped tetragonal zirconia solid solutions. Although the measured total conductivity (σ) for the TiO_2-doped tetragonal zirconia was lower than in undoped tetragonal zirconia solid solution supporting, thus, the above statement but the activation energy values calculated for the conduction process was very similar in both cases, see Table 3. From all the above it seems evident that further investigations are necessary to clarify the electrical behaviour in air of these tetragonal zirconia solid solutions.

If it is taken into account the experimental behaviour of tetragonal zirconia solid solutions in reducing conditions, see Fig. 7a–c, a different analysis of the oxygen partial pressure dependence of the conductivity for undoped and titania doped zirconia samples has to be made. In Fig. 7a the 12 Ce–TZP sample displayed only

two distinct regions: a domain independent of oxygen partial pressure, and a second region dependent of the oxygen activity. Both the electrical conductivity and the threshold oxygen activity for oxygen partial pressure dependence increased with temperature. As it can also be seen the slopes at all experimental temperatures were near to –1/6 in close agreement with that previously predicted [16, 26], and are supporting the idea of a *n*-type semiconduction behaviour at these oxygen partial pressure conditions. It seems clear that the departure from stoichiometry was sufficiently great to develop the characteristic *n*-type conductivity of pure CeO_2 with fullness. This whole of results enables us to state an oxygen vacancy conduction mechanism in the first region, see Fig. 7a, and a higher amount of reduced Ce^{4+} to Ce^{3+} giving rise to a *n*-type electronic conductivity by hopping of electrons between Ce^{4+} and Ce^{3+} cations (small-polaron-hopping mechanism), in the second one.

Although these two same oxygen dependency regions are present in TiO_2-doped tetragonal zirconia solid solutions, however in the *n*-type conductivity region different slopes were displayed as the titania concentration and temperature increased, see Fig. 7b and c. Under moderately reducing conditions (between 10^{-8} and about 10^{-14} Pa) and up to or below 800 °C, the samples exhibited a clear –1/6 dependence of the electrical conductivity on oxygen partial pressure. However, in the most reducing conditions and above 800 °C the slopes are not close to –1/6. The slopes changed towards higher values as the temperature increased see Fig. 7c. From the above oxygen partial-pressure dependence of electrical conductivity measurements, the electronic *n*-type conductivity increases with both titania concentration and temperature and decreasing oxygen partial pressure (below 10^{-14} Pa and above 800 °C) indicating that the *n*-type conductivity is mainly controlled by the Ce'_{Zr} defects concentration. Although the activation energy for the electron mobility was not calculated, but the trend of the log σ vs log pO_2 curves below 800 °C showed a proportionality close to –1/6 which supported the above statement. In a first approach we can conclude that the *n*-type electronic conduction at these specific conditions takes place by a hopping of electrons between Ce^{4+} and Ce^{3+} cations, i.e., by the small-polaron-hopping mechanism. Above 800 °C and oxygen partial pressure lower than 10^{-14} Pa, it seems that a new contribution to the electronic *n*-type conductivity is taking place and the slopes changes again. Such behaviour is clearer in the 10 TiO_2–TZP sample below 900 °C, see Fig. 7c. This indicates that a Ti^{4+} to Ti^{3+} reduction occurred at these conditions with an important contribution to the total conductivity. As reported elsewhere [27] the reduction of TiO_2 is only significant above 830 °C and below 10^{-10} Pa. It is believed that the additional oxygen vacancies created upon the formation of Ti^{3+} cations and the corresponding Ti–Vö association formation depressed the oxygen-ion vacancy mobility. At 900 °C and an oxygen partial pressure of only 10^{-6} Pa the slope of the log σ vs. log pO_2 was higher than –1/4. These results suggested that both Ce'_{Zr} and Ti'_{Zr} defect concentrations are the dominant contributor to the conduction process. Similar results were also found in the titania-doped YSZ and terbia–YSZ systems [18,19].

It is not the scope of the present work to establish a conduction model for these type of mixed conductors, but it is clear that more investigation in the specific case of TiO_2-doped ceria tetragonal zirconia mixed conductors would help to clarify the conduction behaviour of these ceramic materials and, thus, to establish their technological possibilities of application as an electrode in SOFC devices.

5. Summary and conclusions

The single-phase tetragonal structure is retained in 12Ce–TZP containing up to 10 mol% TiO_2 and below 1450 °C. For higher both titania concentration and sintering temperature new phases as zirconium titanate (ZT) and pyrochlore ($Ce_2Zr_2O_7$) appeared. The lattice parameters a_t and c_t of these tetragonal solid solutions decrease and increase, respectively, with titania content and in spite of the strong increasing tetragonality, c_t/a_t, the tetragonal structure as single-phase was retained at room temperature.

The incorporation of titania into ceria-stabilised tetragonal zirconia decreases the ionic conductivity in air of the formed ternary tetragonal zirconia solid solutions with increasing titania content. It is believed that such a conductivity decrease is due to the formation of oxygen vacancy-cation associations (Ti–Vö) with a low vacancy diffusion dynamic resulting, thus, in a decrease in the global concentration of moving oxygen vacancies.

As a function of the oxygen partial pressure, the undoped solid solution exhibited two well-developed regions. At moderately reducing conditions ($>10^{-9}$) an oxygen independent range in which the conductivity is entirely ionic, and an oxygen dependent domain for lower oxygen partial pressure displaying an *n*-type semiconduction behaviour in which the concentration of electronic charge carriers, n, was correlated to pO_2 as $n \propto pO_2^{-1/6}$ in all the experimented range of temperatures and oxygen partial pressures.

For TiO_2-doped samples the electrical behaviour was different to the undoped samples only in that concerning to the most reducing conditions. Below 10^{-9} Pa and up to 800 °C the total conductivity seems to be controlled by the Ce'_{Zr} defect concentration, and the slope log σ-log pO_2 correlates well with a $pO_2^{-1/6}$ dependence. Above 800 °C and with decreasing oxygen partial

pressures a strong departure from stoichiometry with the reduction of Ti^{4+} to Ti^{3+} seems to take place, and the slope increased up to a value close to –1/4, or higher i.e. the theoretical correlation for electronic conduction was $n \propto pO_2^{-1/4}$. This indicates that the conduction process is controlled by the Ce'_{Zr} and Ti'_{Zr} defect concentrations. Assuming that the electrons are located on cerium and titanium sites, the electrical conduction occurs by hopping of the electrons between Ce^{4+} and Ce^{3+} and Ti^{4+} and Ti^{3+} via a small polaron hopping mechanism.

Acknowledgements

This work has been supported by CICYT Project MAT 97–0679-C02–01.

References

[1] H. Iwahara, High temperature proton conducting oxides and their applications to SOFC and steam electrolysers for H_2 production, Solid State Ionics 28–30 (1988) 573–578.
[2] A.O. Isenberg, Energy conversion via high-temperature SOFC, Solid State Ionics (1981) 3–4.
[3] H.S. Isaacs, Zirconia fuel cells and electrolysers, in: A.H. Heuer, L.W. Hobbs (Eds.), Advances in Ceramics, Vol. 3, Science and Technology of Zirconia, The Am. Ceram. Soc. Inc., Columbus, OH, 1981, pp. 406–418.
[4] B. Cales, J.F. Baumard, Mixed conduction and defect structure of ZrO_2–CeO_2–Y_2O_3 solid solutions, J. Electrochem. Soc. 131 (1984) 2407–2413.
[5] H.L. Tuller, Ionic and mixed conductors: materials design and optimization, in: Proc. of 17th Riso Int. Symposiun on Materials Science: High Temperature Electrochemistry: Ceramic and Metals, Riso National Lab, Roskilde, Denmark, 1996, p. 139.
[6] O. Yamamoto, Y. Takeda, R. Kand, M. Noda, Perovskite-type oxides as oxygen electrodes for high-temperature SOFC, Solid State Ionics 22 (1987) 241–246.
[7] H.L. Tuller, S. Kramer, M.A. Spears, Solid electrolyte-electrode system for an electrochemical cell, U.S. Patent No. 5.403, 461, April 4, 1995.
[8] S.A. Kramer, M.A. Spears, H. Tuller, Method for making an electrochemical cell, US Patent No. 5.509, 189, April 23 1996.
[9] B.C.H. Steele, P.H. Middleton, R.A. Rudkin, Materials science aspects of SOFC technology with special reference to anode development, Solid State Ionics 40–41 (1990) 388–393.
[10] F. Capel, PhD thesis, Complutense University of Madrid, 1998.
[11] F.M.B. Marques, G.P. Wirt, Oxygen fugacity in non-flowing atmospheres: I, experimental observations in CO/CO_2 and O_2/N_2 mixtures, J. Am. Ceram. Soc. 75 (1992) 369–374.
[12] V. Longo, Minichelli, X-ray characterization of $Ce_2Zr_3O_{10}$, J. Am. Ceram. Soc. 56 (1973) 600.
[13] C.J. Howard, B.A. Hunter, D.J. Kim, Oxygen position and bond lengths from lattice parameters in tetragonal zirconias, J. Am. Ceram. Soc. 81 (1998) 241–243.
[14] G.S.A.M. Theunissen, Microstructure, fracture toughness and strength of ultrafine tetragonal zirconia ceramics, PhD thesis, University of Twente Enschede, The Netherlands, 1991.
[15] P. Butler, R.K. Slotwinski, N. Bonanos, J. Drennan, B.C.H. Steele, Microstructural-electrical property relations in high conductivity zirconias, in: N.R. Claussen, M. Rühle, A.H. Heuer (Eds.), Advances in Ceramics, Vol. 12, Science and Technology of Zirconia. II, The Am. Ceram. Soc. Inc., Columbus, OH, 1984, pp. 572–584.
[16] F.A. Kroger, The Chemistry of Imperfect Crystals, Vol. 2, American Elsevier Publishing Corporation, New York, 1974, p. 40.
[17] R.E.W. Casselton, Electrical conductivity of ceria-stabilized zirconia, Phys. Status Solidi (A) 1 (1970) 787–794.
[18] K.E. Swider, W.L. Worrell, Electronic conduction mechanism in yttria-stabilized zirconia–titania under reducing atmospheres, J. Electrochem. Soc. 43 (1996) 3706–3711.
[19] P. Han, W.L. Worrell, Mixed oxygen ion and *n*-type conductivity in yttria-stabilized zirconia containing terbia, J. Electrochem. Soc. 142 (1995) 4235–4246.
[20] J.A. Kilner, B.C.H. Steele, Mass transport in anion-deficient fluorite oxides, in: Nonstoichimometric Oxides, Academic Press Inc, New York, 1981.
[21] P. Duran, M. Gonzalez, C. Moure, J.R. Jurado, C. Pascual, A new tentative phase equilibrium diagram for the ZrO_2–CeO_2 system in air, J. Mater. Sci. 25 (1990) 2335001–2335006.
[22] P. Li, I.W. Chen, J.E. Penner-Mahn, Effect of dopants on zirconia stabilization. An X-ray absorption study: II Tetravalent dopants, J. Am. Ceram. Soc. 77 (1994) 1281–1288.
[23] V.C. Pandolfelli, W.M. Ranforth, R. Stevens, Tetragonal zirconia polycrystals in the ZrO_2-TiO_2-CeO_2 system, in: G. De Wit, R.A. Terpstra, R. Metselaar (Eds.), Proceedings of the 1st European Ceramic Society Conference, Elsevier Science Publishing, New York, 1989, pp. 161–165.
[24] P. Durán, F. Capel, C. Moure, A.R. Gonzalez-Elipe, A. Caballero, M.A. Bañares, Mixed (oxygen ion and *n*-type) conductivity and structural characterization of titania-doped stabilized tetragonal zirconia, J. Electrochem. Soc. 146 (1999) 2425–2434.
[25] H. Arashi, H. Naito, Oxygen permeability in the ZrO_2–TiO_2–Y_2O_3 system, Solid State Ionics 53–56 (1992) 431–435.
[26] R.F. Reidy, G. Simkovich, Electrical conductivity and point defect behaviour in ceria-stabilized zirconia, Solid State Ionics 62 (1993) 85–97.
[27] K.E. Swider, W.L. Worrell, Electron paramagnetic resonance of titanium impurities in reduced yttria-stabilized zirconia, J. Am. Ceram. Soc. 78 (1995) 961–964.